POAC'15
Trondheim, Norway

Proceedings of the 23nd International Conference on
Port and Ocean Engineering under Arctic Conditions
June 14-18, 2015
Trondheim, Norway

LABORATORY EXAMINATION OF ICE LOADS AND EFFECTS ON CONCRETE SURFACES FROM BI-AXIAL COLLISION AND ADHESION EVENTS

Jochen Tijsen [1], Steve Bruneau and Bruce Colbourne [2]
[1]Delft University of Technology, Netherlands
[2] Memorial University Newfoundland, Canada

ABSTRACT
Concrete structures in marine environments subject to sea ice interaction are at risk of erosion and damage. Industry is interested in characterizing the ice abrasion phenomenon so that abrasion risk can be managed. The experiments conducted in this work have an exploratory character in order to identify the abrasion phenomenon and qualitatively observe the corresponding processes. The tests are a simulation of micro scale ice-structure interaction and involve the translation of concrete samples while subject to lateral impingement of conical ice samples. Loads in both axes are measured so that tangential and normal force relationship can be examined while the ice samples are catastrophically crushed. The paper divides the interaction into abrasive loading regions and loading orders intentionally to facilitate analysis of the abrasion process. The wear of the concrete surface is described using visual observation and surface feature measurements Concrete of varying mixtures has been examined and the effects on the concrete surfaces from repeated static ice-bonding and bond-breakage is analysed.

INTRODUCTION
Ice abrasion is known to induce wear on concrete offshore structures in the cold environment. The outer layers of concrete can be abraded or protection layers can be torn off by hundreds of kilometres of ice movement each year in sub- and high Arctic regions. Reinforcement and inner bearing strength of the concrete structure are thus under threat. At present, the severity of the problem is not well understood, although some studies have been conducted (Janson J., 1989; Huovinen S., 1990). It is worthwhile to achieve an improved fundamental understanding of the elements of the ice-concrete abrasion process, on the one hand abrasive ice loading and the other hand concrete abrasion resistance. The paper describes an experimental approach and touches upon the knowledge gaps remaining.

EXPLORATORY EXPERIMENT
Ice-structure simulation
The experiment is an exploratory 2D simulation of an ice-structure interaction. The lab scale apparatus provides a simple and controllable analog of the full scale interaction as shown in Figure 1. The entire apparatus is located in a large coldroom at constant ambient temperature of -10 °C.

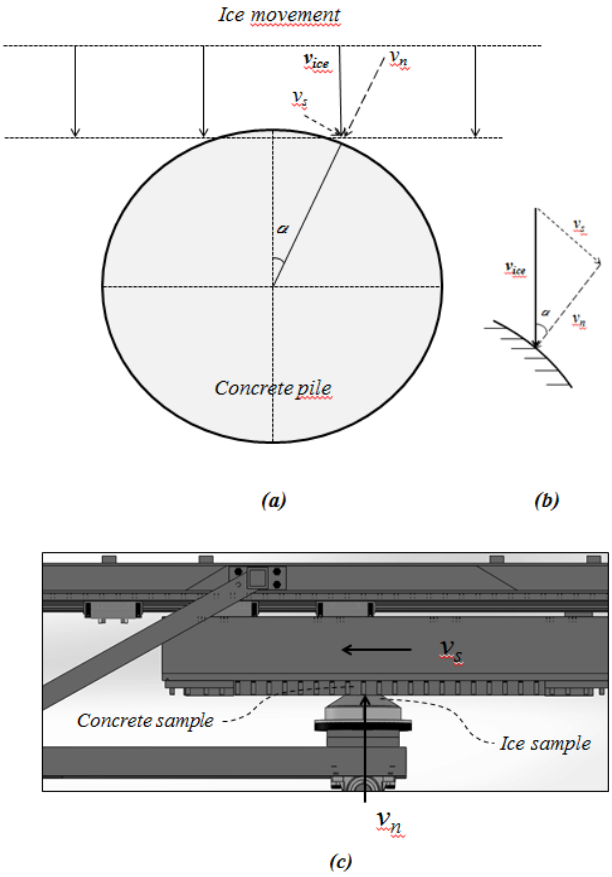

Figure 1 Ice-structure interaction (a) and (b), simulation in the laboratory (c).Figure (a) shows an incoming sheet of level ice with ice velocity (v_{ice}) into a circular concrete pile at a point of contact. (b) shows an schematization on local level. The system has two degrees of freedom: ice velocity (v_{ice}) and angle of contact (α) , together define the normal velocity (v_n) and sliding velocity (v_s). Figure (c) shows the impingement of the conical ice sample (v_n) and simultaneous sliding of the concrete sample (v_s).

The input for the test settings consist of a normal and sliding velocity. The definition of the normal velocity (v_n) is:

$$v_n = v_{ice}\cos(a) \quad (1)$$

The definition of the sliding velocity (v_s) is:

$$v_s = v_{ice}\sin(a) \quad (2)$$

Each individual test run involves impinging a 30 degree conical ice sample on concrete material and in some tests simultaneously sliding the concrete. The description of the ice fabrication procedure is shown in (Bruneau S. et al., 2012). The experiment involves two concrete samples, one high performance and one low performance mixture. The experiment consists of two concrete samples of 1495x195x207 mm. An high performance and a low performance concrete grade according to the concrete mixtures in Table 1. The high performance (HP) concrete sample consists of a marine concrete grade ($\sigma_c \approx 70$ MPa). Silica fume is part of the HP mixture and result into a larger matrix strength. The pore spaces fills up

with the very fine silica fume particles and increases the cohesion of the concrete. The finish of the silica fume causes a very smooth surface. The low performance (LP) concrete sample is a lower concrete grade ($\sigma_c \approx 40$ MPa). The surface of the LP concrete was rougher than that of the HP concrete despite the same level of formwork being used to fabricate the concrete grades. The intention of the LP concrete sample is to make it abrasion sensitive and use the output data as reference concrete.

Table 1 Concrete mixtures

	HP Concrete Sample	LP Concrete Sample
Air volume	3 – 5%	3 – 5%
SCM	8%	0%
Binder	500	300
C/F	1.2	1.2
W/B	0.33	0.5
Absorption	0.01	0.01
Portland cement	460	300
SF	40	0
C.A (8 – 16 mm)	952.09	1070.39
F.A (0 – 8 mm)	793.41	891.99
W	165	150
TW	182.46	169.62

The test sequence for each concrete sample involves solely crushing (v_{ice} = 0.1; 1.0 and 10.0 mm/s), solely sliding (v_{ice} = 1.8 and 180.0 mm/s / normal force F_n = 10 kN) and simultaneous crushing and sliding for three chosen angles of contact.

Data logging

Load cells log forces and displacement sensors log the displacements in the normal and sliding directions. A SLR camera, three video cameras (front, side and back) and a High-speed camera (side view / 50 – 150 FPS) record the concrete surface and ice samples during testing. Also, a thermal image record behind the interaction gives the signature of heat traces after interaction on the concrete surface.

There is currently no standard definition or measure of concrete abrasion due to ice action. This paper defines abrasion as concrete surface texture change due to mass loss. This study explores four ways of quantification of concrete abrasion:

- Visual data by video and photo camera
- Surface roughness measurement device (up to 160 μm)
- Two identical test runs before and after a test sequence. Identify potential change of tangential forces due to the change of surface texture.
- Calliper (hole characterization)

RESULTS AND DISCUSSION

General: Point of Contact

The test sequences align with the idea of three typical adhesive regions as shown in Figure 2, because three typical abrasive ice loading regimes occur over varying angles of contact (α).

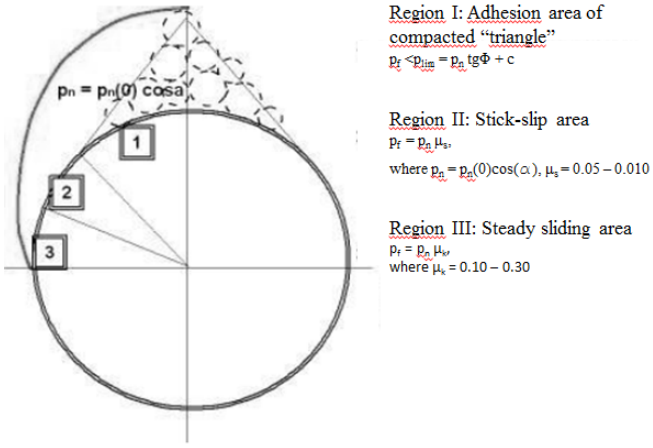

Figure 2 Contact regions with different abrasion mechanisms according to (Jacobsen et al., 2012)

The abrasion mechanisms globally consist of three categories as is shown in Figure 2: Solely crushing ($\alpha \approx 0^{\circ}$), crushing and sliding ($0^{\circ} < \alpha < 90^{\circ}$) and solely sliding ($\alpha \approx 90^{\circ}$) . These regions correspond to the three following modes of interaction:

- Region I 'Crushing and extrusion'
- Region II 'Stick-slip'
- Region III 'Slip'

The type of loading gets even more interesting on micro scale level, because each loading type may contribute in its own unique manner to concrete abrasion. (Itoh Y. et al., 1988; Huovinen S., 1990; Bekker A. et al., 2010; Sistonen E. and Vesikari E., 2008; Jacobsen et al., 2012) and a few others already identifies 9 abrasive loading types, all contributing to abrasion according to one of the following orders:

- Primary order of loading: Direct exceedance of abrasion strength by loading and physical deterioration of material surface occurs: Shear stress due to tangential forces (friction and adhesion).
- Secondary order of loading: Reduction of abrasion resistance and thus increasing the probability of physical deterioration of material surface: Stick-slip cycles, indentation pore pressure, freeze-thawing cycles, concrete shrinkage, thermal gradients, chloride migration, dissolving of lime.

Region I 'Crushing and extrusion':

The location associated with Region I abrasion is around the structural face perpendicular to the ice movement and involves most critical ice abrasion on offshore structures (Janson J., 1989; Hara F. et al., 1995). The largest local compression (Bekker A. et al., 2003) and shear stresses occur in this region and result into exceedance of the abrasion resistance of the concrete. The local compression stress under brittle ice failure may reach, for very short periods, up to 60 MPa for multiyear sea ice (Masterson D. et al., 1993) or in small-scale laboratory conditions over 100 MPa at areas of a few mm^2 (Mackey T. et al., 2007) and corresponding friction processes can thus induce large shear stresses. The observation of eruption of spalls during fast tests *($v_n > 1.0$ mm/s)* resembles an extrusive processes under extreme compression stress (Jordaan I., 2001).

The abrasive ice loading quantity in this paper is work (or energy), because (Itoh Y. et al., 1988) shows, through empirical data, proportionality between concrete abrasion on the one hand and normal pressure and ice sliding distance on the other hand. Work includes force and displacement through a proportional relation and is thus able to indicate a global abrasive load. Also, one is able to determine the cumulative loading and compare it to the abrasion depth. The formula for work in normal direction is:

$$W_n = \int_0^x F_n(x)\,dx \approx \sum_i^{n-1}(x_{i+1} - x_i)\left(\frac{F_{n,i+1}+F_{n,i}}{2}\right) \quad (3)$$

Where x is the indentation (mm), F_n the normal force (kN) and i the index number of a chosen sample. The discrete approximation of the continuous integral is the trapezoidal integration rule. The formula for work in the sliding direction is:

$$W_s = \int_0^x F_s(x)\,dx \approx \sum_i^{n-1}(z_{i+1} - z_i)\left(\frac{F_{s,i+1}+F_{s,i}}{2}\right) \quad (4)$$

Where z is the sliding distance (mm), F_s the tangential force (kN) and i the index number of a chosen sample. The work is spread over the contact area such that it normalizes the loading. The unit of the abrasive loading is J/mm^2 per mm absolute sliding distance, where absolute means the apparatus' reference system. Figure 3 shows the change of surface texture and loading data shows the change of cumulative abrasive loading from tests that correspond to Region I loading. In these cases the ice was crushed against the concrete sample without lateral sliding.The change in cumulative loading and abrasion reveals aspects of the abrasion process.

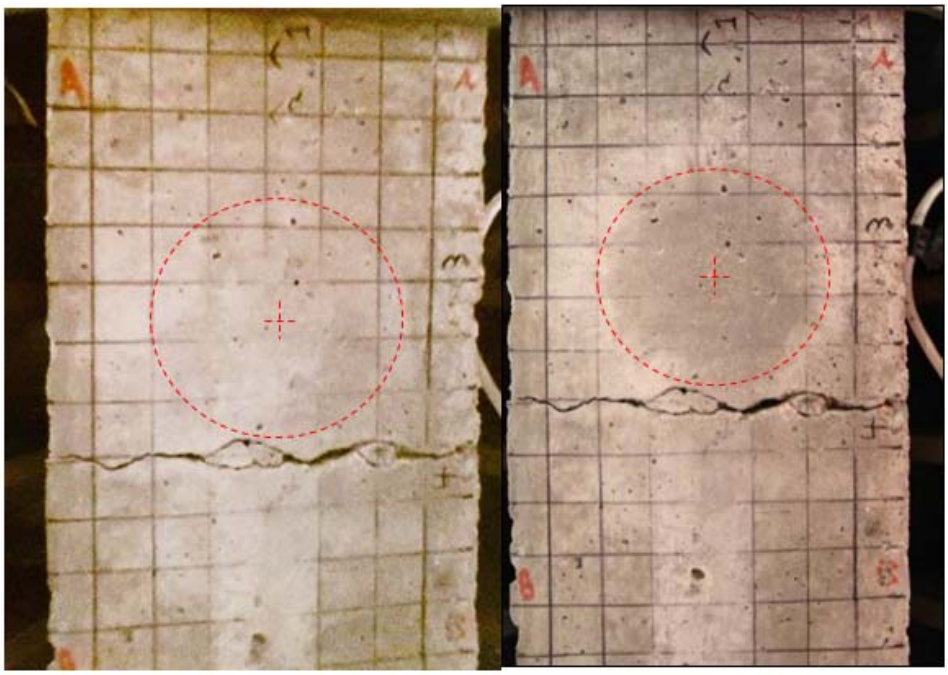

Figure 3 Surface of high performance concrete sample before (left) and after (right) slow crushing test (v_{ice} = 0.1 mm/s / $\alpha \approx 0^\circ$). The abrasive loading over only one test run is about 1.95 J/mm^2 normal loading at the reference cross. The loading correspond to a nominal compression pressure of about 20 MPa. The concrete after the test shows scour like traces radial on the concrete surface and also involves exposure of small aggregates.

Region II 'Stick-slip'

The stick-slip region doesn't abrade the concrete in an early stage, but will reduce the concrete abrasion resistance over long time scales. Figure 4 shows a stick-slip cycle and indicates static friction up to half (5 kN) the normal force (10 kN). The stick-slip region can abrade the concrete surface due to local fatigue issues (Huovinen S., 1990). Stick-slip loading falls thus under the secondary order of abrasive loading, because it doesn't exceed the nominal surface abrasion resistance but does tend to reduce it over time.

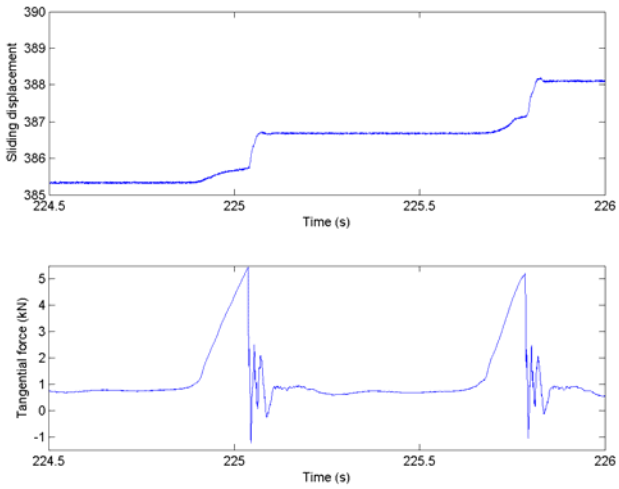

Figure 4 Stick-slip cycle for 1.8 mm/s sliding rate under 10 kN normal load – High performance concrete sample

Figure 5 shows that the stick-slip character depends on ice velocity and the stick-slip region thus reduces with increasing ice velocity. Slow ice velocities v_{ice} are of increasing importance for the local fatigue strength of the concrete surface.

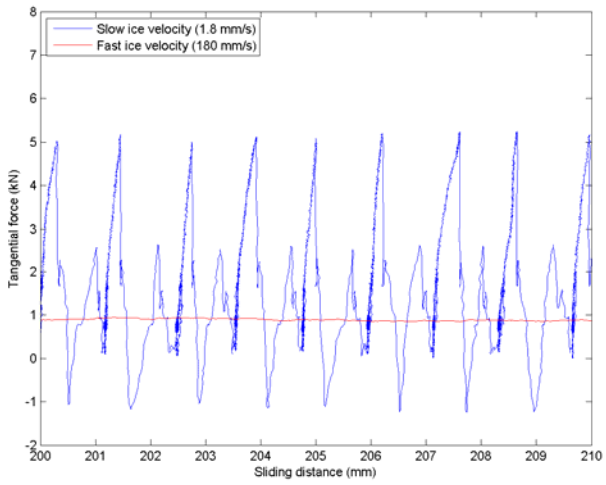

Figure 5 Tangential force for slow (v_s=1.8 mm/s) and fast sliding (v_s=180 mm/s) under 10 kN normal load – High performance concrete sample. The fast ice velocity is a very smooth sliding process in comparison with the slow ice velocity. The scatter of data points originates from the overshoot of the position in sliding direction. Figure 4 correspond with the slow ice velocity and illustrates the stick-slip cycle over time instead.

The stick-slip cycle period not only depends on the ice velocity (v_{ice}) and angle of contact (α), but also on the concrete type. Note the stick-slip period also depends on the stiffness of the apparatus, but is the same for all tests. Figure 6 and Figure 7 are FFTs of the tangential loading in identical tests, but the two figures compare high performance and low performance concrete. The peak frequency and active frequencies vary (HP Concrete grade: f_{peak}≈0.7 Hz / LP Concrete grade: f_{peak}≈0.78 – 0.85 Hz), the LP concrete involve higher active frequencies than the HP concrete and indicate a variation in adhesive properties of the two concrete types. The (smooth) high performance concrete sample is more sensitive (lower active frequencies) for adhesion than for the (rough) low performance concrete sample. Adhesive bonding depends mainly on real contact area (Saeki H., 2010) and increases with increasing roughness. The adhesive forces seem to be larger on a smooth surface than rough surface over a test run, corresponding to observations on confinement in (Dragt R., 2013) for varying roughness' in ice-steel crushing tests. Ice seems to adhere between two asperities on the rougher surface and thus reduce the real contact area.

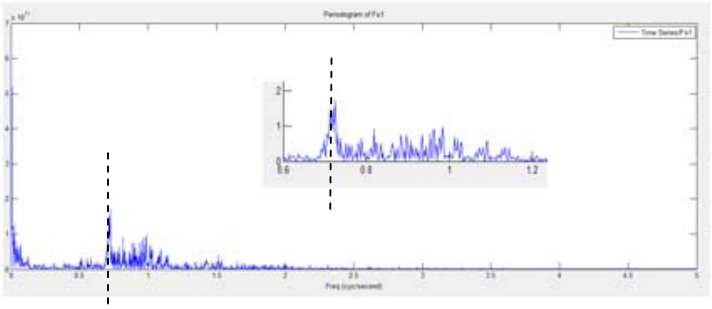

Figure 6 High performance concrete sample – FFT of tangential force under slow ice velocity (v_{ice}= 1.8 mm/s) at α=86.6 degrees, from 0 – 5 Hz. The peak frequency concentrates about 0.7 Hz.

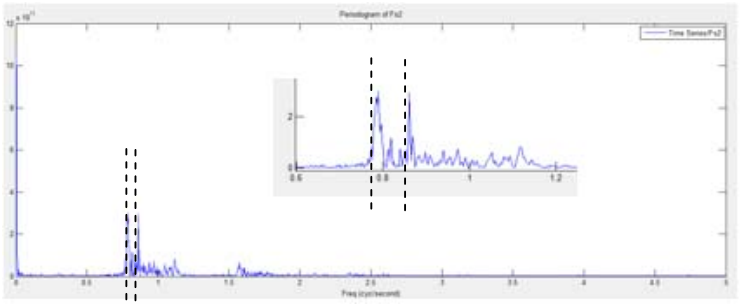

Figure 7 Low performance concrete sample – FFT of tangential force under slow ice velocity (v_{ice}=1.8 mm/s) at α=86.6 degrees, from 0 – 5 Hz. The peak frequency concentrates at about 0.78 – 0.85 Hz.

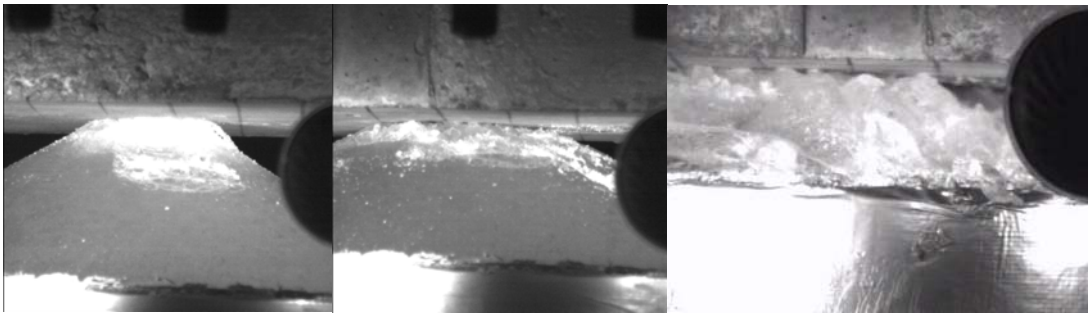

Figure 8 High speed imagery at varying contact areas, the screenshots show beginning test 1.5 Hz (left photo), halfway test 0.9 Hz (middle photo) and at the end of the test 1.1 Hz (right photo).

Figure 8 shows that the stick-slip period depends on fracture and thus on real contact area. High frequency motions correspond with low static binding and low frequency motions with high static binding. The ice sample in the right photo shows reduced real contact area due to fracture and spalling, and the stick-slip frequency is thus increased.

Region III 'Slip'

The slip region doesn't critically affect the abrasion risk of the concrete significantly. Low stresses and large sliding velocities characterize the region barely leaving any abrasion traces behind. However if we consider that the first two regions should not govern the design abrasion loading, then ice sliding can cause abrasion over long sliding distances as is shown in (Itoh Y. et al., 1988) and (Bekker A. et al., 2011). The lower stress cases do require sufficient localized compression stress to induce abrading effects, for example due to enclosed ice spalls and rubble at the free surfaces between ice sheet and structure. The slip region only has to overcome the dynamic ice-concrete friction during large ice velocities and the tangential force consists of a combination of wet and dry friction. The slip region changes into a stick-slip region for lower ice velocities.

Observations of ice abrasion

Figure 9 Concrete abrasion on the high performance concrete sample (left) and low performance concrete sample (right) over a test sequence. The location is at the starting point of the test runs as shown with the cross in Figure 3. The loading on the high performance concrete sample is much higher than for the low performance concrete sample. The grid lines (20 mm distance) provide reference.

Figure 9 shows initial traces of abrasion at the start location (z_{ab} = *94 mm*) over a test with crushing and sliding that exhibited stick-slip behaviour. The abrasion damage is minor in comparison to field studies (Janson J., 1988). The abrasion loading was over W_n = 2.6 J/mm^2 and W_s = 0.2 J/mm^2 for the HP concrete and less for the low performance concrete. The high performance concrete sample shows less abrasion than the low performance concrete sample, the silica fume particles seem to increase the matrix strength and improve the abrasion resistance. Also, the surface reveals smaller aggregates already exposed, indicating the cement layer is wearing. The concrete surface evolves over longer ice sliding distances and exposes, in a later stage, larger diameter aggregates (Itoh Y. et al., 1988; Huovinen S., 1990). Thus, the cement properties seem to govern the initial abrasion rate in Figure 9.

The tangential force for two identical sequential tests didn't show any significant variation. The surface texture measurement device could only measure a maximum surface elevation of 160 µm, thus we can state the local abrasion of the high performance concrete sample is larger than 160 µm. The calliper helps to describe the surface visually, with more details in (Tijsen J., 2015).

Interface layer

The interface layer is the layer between the undamaged ice and concrete and involves a mixture of crushed ice and concrete particles. The crushed ice particles originate from flaking ice during sliding due to micro shearing. The concrete particles originate from flaking concrete due to microshearing, but also due to adhesion with the ice. The mass flow on the interface under high pressure exhibits a hydrodynamic character and under lower pressures shows a more solid granular character (Jordaan I., 2001). The liquefaction of ice is due to a combination of pressure and frictional heat. The ice surface layer will immediately absorb frictional heat for melting a very thin surface sub-layer and during refreezing release the latent heat. Figure 10 shows enclosure of concrete particles after recrystallization of the ice surface (shown by the fine crystalline ice structure) and Figure 11 shows evidence of heat traces. Also, Figure 10 shows the ice roughness increases during interaction due to the enclosure of concrete particles, and thus the abrasion rate increases in a similar manner as in (Itoh Y. et al., 1988) due to the effect of sand particle content in the ice.

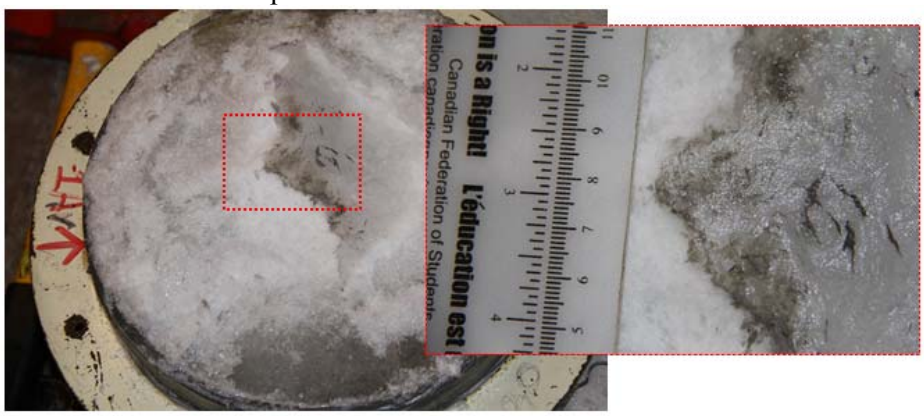

Figure 10 Concrete dust and particles enclosure under recrystallized ice after test 1a (v_n = 1.0 mm/s / v_s = 18.0 mm/s) at the high performance concrete sample

Fast moving ice generates frictional heat as is shown in (Tijsen J. et al., 2013). With increasing melting of ice, hydrodynamic characteristics at the contact dominate over asperity contact in governing the characteristics of the interface layer and thus abrasion rates. Lower temperatures imply less melting and increasing dry friction over wet friction. The ambient

temperature during testing was -10 (+-1.5) ˚C and shortly after interaction temperature increments of +10.3 ˚C were measured as shown in Figure 11. The heat traces indicate very local interaction and possible liquefaction of the ice interface material.

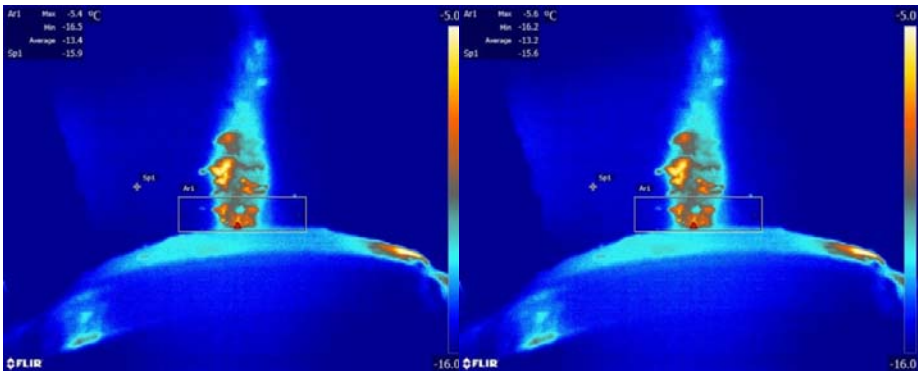

Figure 11 Thermal image of a crushing and grinding test (at α=86.6 deg and ice velocity 18 mm/s) concrete (emittance = 0.92 – left picture) and for ice (emittance = 0.96 – right picture) temperature data

Temperature increments on the interface will also reduce the adhesive bonding (Saeki H., 2010) and thus tend to increase the stick-slip frequency. Large local temperature gradients due to heat generation can also introduce thermal stresses in the concrete surface. Thermal stresses reduce the strength of the concrete surface and will increase the probability on local abrasion.

CONCLUSIONS

The experimental set-up is suitable for simulation of two-dimensional ice-structure interaction on and examination of local material processes like ice abrasion. The most important advantage is the ability to simulate interaction at a predetermined Point of Contact dependent on angle (α). The most important drawback is the limitation of not being able to easily achieve large ice sliding distances.

Observations from the preliminary laboratory tests discussed here indicate that:

- The type of abrasive ice loading depends on ice velocity (v_{ice}) and Angle of Contact (α) (AoC). The paper distinguishes Region I: 'Crushing and extrusion' ($\alpha \approx 0^{\circ}$), Region II: 'Stick-slip' ($0^{\circ} < \alpha < 90^{\circ}$) and region III: 'Slip' ($\alpha \approx 90^{\circ}$).
- Region I: 'Crushing and extrusion' experience the highest level of abrasion from all regions.

On adhesion:

- The component of local static bonding during a sliding test on the high performance concrete sample can be up to half of the compression force.
- Adhesion introduces a cyclic load on the concrete surface due to stick-slip under low ice velocities (v_{ice})
- The stick-slip cycle depends on real contact area. Ice fracture and spalling reduces adhesion bonding due to reduction of real contact area.
- The areal size of region II: 'Stick-slip' reduces with increasing ice velocity (v_{ice})
- Static bonding increases with decreasing concrete surface roughness. Surface characteristics of concrete like roughness depend on concrete mixture composition, for example cement type or additives like silica fume.

On micro scale processes:

- Secondary order abrasive ice loading only becomes of importance on long sliding distances, which is often the case with lifetime design in offshore structures.
- Frictional heating in combination with contact pressure significantly increases the temperature of the ice-concrete interface. The local temperature gradients can affect the character of the local shear loading (hydrodynamic flow versus granular solid flow)
- Frictional heat generation introduces local thermal stresses within the concrete surface and reduces the abrasion resistance.
- The ice surface material crushes and recrystallizes an ice-concrete mixture during interaction.
- The ice roughness increases due to enclosure of concrete particles in the ice surface.
- The high performance concrete sample shows a better abrasion resistance than the low performance concrete sample, most likely due to an improved binding strength due to the addition of silica fume.

Thus, the experimental setup is able to provide valuable data on microscopic processes. The authors refer for the interested reader to the underlying master of science thesis (Tijsen J., 2015) for more details.

ACKNOWLEDGEMENTS

The authors are thankful to the STePS^2 group within Memorial University Newfoundland (MUN) for funding. Second, to the team of lab technicians of MUN to provide best support possible in building and operating the tests. Last, appreciation goes to the Arctic group within Delft University for providing fruitful discussion on underlying master thesis work.

REFERENCES

- Bekker A. et al., 2003, Abrasion Effect of Ice Cover on Supports of Hydraulic Engineering Structures in Conditions of Sakhalin Island Shelf, Proceedings of the Thirteenth International Offshore and Polar Engineering Conference
- Bekker A. et al., 2011, Experimental Study of Concrete Resistance to Ice Abrasion, Proceedings of the Twenty-first International Offshore and Polar Engineering Conference
- Bruneau S. et al., 2013, Laboratory indentation tests simulating ice-structure interactions using cone-shaped ice samples and steel plates, Proceedings of the 22nd International Conference on POAC'13.
- Dragt R., 2013. The collision of cone-shape ice samples against steel plates of varying surface roughness, chapter 2. Submission of master of science thesis to the Delft University of Technology, The Netherlands
- Hara F. et al., 1995, Prediction of the degree of abrasion of Bridge Piers by Fresh water ice and the Protective
- Huovinen S., 1990, Abrasion of Concrete by Ice in Arctic Sea, Rakenteiden mekani ikka, Vol. 23 No. 1 1990 s. 23-35
- Huovinen S., 1992, Abrasion of Concrete Structures by Ice, Cement and Concrete Research, Vol. 23, p. 69-82
- Itoh Y. et al., 1988, An Experimental Study on Abrasion of Concrete Due to Sea Ice, OTC
- Jacobsen S. et al., 2012, Concrete Destructure due to Ice-Indentation Pore Pressure, Proceedings of the Twenty-second International Offshore and Polar Engineering Conference

- Janson J., 1987, Results from the winter seasons 1988 – 1989. Conclusion after the three winters 1986 – 1989. Joint Industry Study, Field investigation of Ice Impact on Lightweight Aggregate Concrete
- Janson J., 1989, Report of field investigation of ice impact on lightweight aggregate concrete – results from the winter season 1986 -1987, VBB, Stockholm, Sweden
- Jordaan I., 2001, Mechanics of ice-structure interaction, Elsevier – Engineering Fracture mechanics 68.
- Mackey T. et al., 2007, Experiments on the fracture of polycrystalline ice. Proceedings of POAC 2007
- Masterson D. et al., 1993, Description of multi-year ice indentation tests at Hobson's choice ice island, Proceedings, 12th International conference on offshore mechanics and arctic engineering, vol. 4, Glasgow, p. 145-55
- Saeki H., 2010, Mechanical Properties between Ice and Various Materials Used in Hydraulic Structures: The Jin S. Chung Award Lecture, International Journal of Offshore and Polar Engineering Vol. 21, No. 2, pp. 81 – 90
- Tijsen J. et al., 2013, Use of Thermal Imagery to assess Temperature Variation in Ice Collision Processes, Proceedings of the ICETECH'13 conference.
- Tijsen J., 2015, Ice-concrete abrasion, Submission of a master of science thesis to the Delft University of Technology, The Netherlands.